EUROPEAN ORGANIZATION FOR NUCLEAR RESEARCH

CERN/SPSC 83-44
SPSC/I 146
07.06.1983

LETTER OF INTENT

AN EXPERIMENT TO MEASURE ν_μ-e SCATTERING WITH A LARGE WATER CERENKOV DETECTOR*

P. Bloch[3], A. Blondel[2], J. Feltesse[3], R. Fries[2],
F. Jacquet[2], A. Milsztajn[3], U. Meyer-Berkhout[1],
A. Staude[1], M. Virchaux[3], R. Voss[1].

1. Sektion Physik der Universität, Munich, Germany
2. Ecole Polytechnique, Palaiseau, France
3. CEN, Saclay, France.

* Subject to approval by the National Funding Agencies.

INTRODUCTION

In this letter we present a new method to perform a high statistics ν_μ-e scattering experiment. It is based on the detection of the Cerenkov light emitted by the forward produced electrons in a water target (Ref.1).

In chapter I we recall the physics interest of such an experiment, mainly the precise measurement of $\sin^2\Theta_w$. In chapter II, we present the detection principle and the expected accuracy on angular and energy measurements. The next chapter is devoted to a detailed analysis of background contaminations with a particular emphasis on e/γ and e/π° discrimination. Finally a possible set-up is discussed in chapter IV.

PHYSICS OBJECTIVES.

I-1-The Weinberg angle measurement.

The reactions induced by neutrinos on electrons are a unique tool to study the structure of the weak interactions. The differential cross sections of the purely leptonic neutral current

$$d\sigma/dy\ (\nu_\mu e \to \nu_\mu e) = 2/\pi\ G^2 m_e E_\nu [g_L^2 + g_R^2 (1-y)^2]$$

$$d\sigma/dy\ (\bar{\nu}_\mu e \to \bar{\nu}_\mu e) = 2/\pi\ G^2 m_e E_\nu [g_L^2 (1-y)^2 + g_R^2]$$

(where G is the Fermi constant, m_e the electron mass, E_ν the ν energy and $y = E_e/E_\nu$) depend on the two coupling constants g_L and g_R which are related, in the standard model, to $\sin^2\Theta_w$ by

$$g_L = -1/2 + \sin^2\Theta_w \qquad g_R = \sin^2\Theta_w$$

The measurement of these cross sections yields a value of $\sin^2\Theta_w$ which is basically free of theoretical corrections and in particular independent of any hypothesis on the nucleon structure.

An accurate determination of $\sin^2\theta_W$ provides a test of the renormalizability of the theory (Ref.2) by comparing the Z° mass obtained from lowest order computation ($M_{Z^\circ} = 37.3\text{GeV}/\sin\theta_W \cos\theta_W$) to the real mass which is likely to be measured soon. The electroweak radiative corrections to the Z° mass formulae are of the order of 3 to 5 GeV, corresponding to an apparent change of $\sin^2\theta_W$ by .02 to .03 . Therefore a measurement with an accuracy of $\Delta \sin^2\theta_W = .005$ is necessary.

I-2-Status of the $\nu_\mu e \to \nu_\mu e$ experiments.

The neutrino electron scattering has two main characteristics :

-The cross section is very small ($\sigma \sim E_\nu \ 10^{-42}\ \text{cm}^2/\text{GeV}$, about 10^{-4} of the ν_μ-nucleon reactions). Therefore a large detector is needed to get sufficient statistics.

-The typical angle of the scattered electron is small:

$$\theta_e = \sqrt{2m_e/E_e\ (1-y)} \leq 32\text{mrad}/\sqrt{E(\text{Gev})}$$

A very good angular resolution is necessary to separate well the signal from the backgrounds and to minimize the systematic errors.

The bubble chambers have a good angular resolution but, due to their low target mass, their statistics are poor(a few tens events). Counter experiments (Ref. 3) offer larger mass: ~ 100 $\nu_\mu e$ events has been observed in the detector of the CHARM Collaboration. This experiment is however limited by a moderate fiducial mass (~ 80 tons) and by its poor angular resolution (larger than the kinematical limit) which gives a large uncertainty on the background substraction.

A possible improvement is to build a larger calorimeter with a finer grain (Ref.4). We present another approach which offers roughly the same fiducial mass with a three times better angular accuracy.

I-3 Other physics interest.

Although quantitative studies are still in progress, we would like to mention some other physics potentials of the detector. Because of the good angular resolution, much smaller than the kinematical limit, the $E\theta^2$ distribution could be sensitive to the light supersymetric partner of the goldstinos:such new particles would induce an increase of the ν_μ-e cross section at very low Q^2 (Ref.5)

A detector sensitive to electrons or photons at small angles is also well suited to search for new phenomena like neutrino decay ($\nu' \rightarrow \nu\gamma$, $\nu' \rightarrow \nu ee$).

II-THE DETECTION PRINCIPLE.

The proposed detector consists of a large volume of water acting both as a target and Cerenkov radiator. Cerenkov radiation emitted by particles travelling in water is detected by three complementary methods providing both angle and energy measurement, as well as a good electron identification. A veto counter in front and a muon spectrometer behind complete the apparatus.

A $\beta=1$ particle in water gives rise to a Cerenkov light cone with an opening angle of 42°. This light, detected by photomultipliers, yields an average number of 20 photoelectrons per track per cm. This number, checked experimentally (Ref.6), includes the quantum efficiency of a standard P.M. and the loss due to U.V. absorbtion in 2m water and in a plastic window.

The idea to use this Cerenkov cone has been put forward originally in 1978 by J.W. CRONIN and M.L. SWARTZ (Ref.7). In their proposal the Cerenkov cone is detected through two tilted opposite windows. A small deviation from the forward direction is measured by comparing the amount of light in the two windows. This method is sensitive to correlations between angle and energy measurement.

In our method three independent measurements of the Cerenkov cone are proposed:

1) The forward measurement uses a tilted window, (but with a larger tilt than in the Cronin's proposal) followed by a mirror system which focuses the Cerenkov cone on a photon detector, giving a very precise measurement of the angle and a first estimate of the energy.

2) The inner detector is similar to the Irvine-Michigan-Brookhaven proton lifetime detector (Ref.8) and provides an energy measurement and some pattern information.

3) The "shower scanner", made of angle selective photon detectors, is installed inside the water. It measures the number of small angle tracks at the beginning of the shower and provides separation between electrons and γ-rays.

II-1-Forward detector.

A fraction of the Cerenkov light cone emitted by a small straight segment of a charged track leaves the water through a plane glass window. After refraction, the light is focused by a spherical mirror. The resulting image in the focal plane is almost an arc of circle. The next track segment, if it has the same direction as the preceding one, gives the same picture in the focal plane. In other words, a Cerenkov photon of direction $\vec{k}$ in water, gives a photon of direction $\vec{k}'$ in the air (after passing the window) and gives a point M(z,y) in the focal plane of the mirror. There is therefore a unique relation between the impact point on the focal plane and the direction of the photon in water, independent of the emission point. (Fig. 1). A change of $\vec{k}$ by 1 mrad in a plane perpendicular to the window is amplified by the refraction to a 4 mrad change in $\vec{k}'$, thus reducing the quality requirement on the external optics.

Therefore the arc measurement in the focal plane gives a precise measurement of the projected angle (called θ_z) of the track on a plane perpendicular to the window. The tilt of the window and the size of the forward detector are designed to accept Cerenkov photons emitted by tracks within 25 mrad around the beam axis.

For an electron shower the arc is smeared by multiple scattering. This effect is increased by the bremsstrahlung and pair production processes which decrease the electron energy. However, the shower retains the direction of the primary electron as shown in fig.2 . The number of photons emitted by the charged tracks of the shower at an angle Θ_z is proportional to the electron energy, i.e. the distribution $1/E\,dN/d\Theta_z$ is energy independent (fig.3).

Each individual event gives rise to a distribution of the same shape but with statistical fluctuations, providing for each shower three informations:

i) Θ_z measurement.

The position of the maximum of $dN/d\Theta_z$ is a measurement of Θ_z. Fig.4 shows the $\Theta_{measured} - \Theta_{true}$ distribution for different energies. The resulting error is (Fig.5)

$\sigma(\Theta_z) = 4\text{-}7\ \text{mrad}/\sqrt{E}$

where the higher number corresponds to very pessimistic assumptions about the loss of photons in the optical system.

ii) Energy measurement (E_{For}). The integral over±20mrad of the distribution shown in fig.2 gives a first estimate of the electron energy and, by comparison with the total energy measured in the inner detector, a good particle identification.

iii) The shape of the peak near the maximum is different for electrons, muons and hadronic showers and provides important information for background discrimination by using the height of the peak (E_{Peak})

II-2 The inner detector.

Photomultipliers inside the water, around the fiducial volume,as in the IMB proton lifetime experiment (Ref.8) will give the following informations:

-total energy measurement E_T. With one to three 5" P.M.'s per square meter one obtains 1.5 to 4% coverage. Assuming 2% coverage the number of detected photoelectrons is 200 per GeV. One expects a resolution of $\sigma(E_T)/E_T = 10\%/\sqrt{E_T}$ for electromagnetic and $\sigma(E)/E = 50\%/\sqrt{E}$ for hadron shower.

-Position measurement. The forward detector does not give any information on the position.The inner detector by pattern analysis can give a resolution of $\lesssim$ 10cm.

II-3-The shower scanner.

γ rays from various sources are expected to be one of the major backgrounds, as well as the signature for new exciting phenomena.

Photons and electrons differ only in the first part of the shower and their separation requires the isolation of the photons emitted in the first half radiation length of the track: As soon as the shower develops, wide angle tracks are produced, emitting a halo of Cerenkov light. This halo contributes to the resolution in total energy, but prevents from isolating with the inner detector the photons emitted by the first part of the shower.

The problem is solved by selecting the Cerenkov photons emitted in a narrow angular interval. A possible device, sketched in the fig.6, detects photons emitted by tracks within 100mrad around the beam axis. Four rows of such selective P.M. will be used to discriminate e from γ rays (see section III-3). An average of 16 photoelectrons per 12cm of track (1/3 of X_0) are collected.

III-SELECTION OF THE EVENTS-BACKGROUND.

III-1 Selection of the events.

We have used the M.C. program GAGJET (Ref. 9) for generation of hadronic final states and the program CASCAD (by courtesy of A. Grant), where we have implemented the emission of Cerenkov light, for propagation of electromagnetic and hadronic showers in the water.

Neutrino-electron scattering events will appear as single electron emitted a an angle $\Theta_{e^-} \leq \Theta_{max} = 32 \text{ mrad}/\sqrt{E_e}$, i.e. within the acceptance of the forward detector for electron energies E >2 GeV. The ratios of the number of photons measured in the forward detector (E_{For}) and the number of photons in the peak (E_{peak}) to the total energy (E_T) differ for the various types of particles:

-muons do not shower. The Cerenkov photons emitted by a muon have almost no dispersion in polar angle; they are focused on the same ring, leading only to a narrow peak in $dN/d\Theta$.

-charged pions at zero degree show up as a small narrow peak in the forward detector, due to photons emitted before their interaction, superimposed to a broad background due to the hadronic shower.

-electrons produce the characteristic distribution shown in fig.2.

Fig.8 is a scatter plot of E_{For}/E_T and E_{peak}/E_{For} for 10 GeV muons, electrons, π^+ and π^o's emitted in the beam direction. A cut in this plot which retains 98% of the electrons rejects all the muons and 98.5% of the charged pions. This cut will be referred to in the following as the "standard electron cut".

III-2-Background from deep inelastic scattering on nucleon.

A major source of background is inelastic scattering of ν_μ on nucleons. The cross section is 10^4 time higher than for ν_μ-e scattering. Rejection of these processes relies on the fact that the angular distribution of the final state hadrons is much wider than the angular acceptance of the forward detector. An additional rejection for charged current reactions is obtained from the identification of the muon in the muon spectrometer.

To get a quantitative estimate, we have used our Monte Carlo simulation. It is however impossible to generate 10^5 neutrino events and their hadronic cascade. We have therefore used the following procedure:

Neutral currents

We have first tested the assumption that large angle hadron showers ($\Theta_h > 25$ mrad, the acceptance of the forward detector) do not contribute to the background. For that purpose, we have fully generated 1000 events at $\Theta_h = 20$ mrad and $\Theta_h = 100$ mrad. None of the events survives the standard electron cut. We have then generated 1000 events on the beam axis. A single event survives the cut (fig.8). From that we estimate that the rejection against hadronic showers with $\Theta_h < 25$ mrad is better than $1/(3\times10^{-3})$. Assuming that the remaining background is flat in the $E\Theta^2$ distribution, we get an extra factor 10. Events with $\Theta_h < 25$ mrad correspond to 4% of the total neutral current rate, leading to a signal over background ratio

$$\frac{S}{B_{NC}} > \frac{1}{2\ 10^3} \times \frac{1}{4\ 10^{-2}\ 3\ 10^{-3}\ 10^{-1}} = 40$$

Charged currents

We can divide the charged current events in 3 categories:

i) events with a high energy muon ($E_\mu > 6$ GeV) do not contribute to the signal. The muons are either identified in the muon spectrometer or, if emitted under large angles, by their characteristic pattern in the inner detector.

ii) events with low energy muons under large angles are indistinguishable from neutral current events. They are as frequent as the neutral current events and therefore contribute to the background at the same level (S/B =40)

iii) events with a low energy muon at small angle ($\theta_h \leq 25$mrad), generate a special background since, in the forward spectrometer, the muon peak superimposed on the signal of the hadron shower could simulate an electron. Assuming that a muon with an energy above 3 Gev, corresponding to a range of 18 absorption lengths,will be identified in the inner detector, these events amount to 10^{-4} of the charged current rate. The standard electron cut gives a rejection of at least 10. Combining with the $E\Theta^2$ cut, we obtain :

$$\frac{S}{B} \geq \frac{1}{10^4} \times \frac{1}{10^{-4} \times 10^{-1} \times 10^{-1}} = 100$$

III-3 Coherent production. γ, π° and electron separation.

It has been pointed out recently that a large background to the $\nu_\mu e$ signal can be produced by coherent processes, for example the coherent production of π°'s(Ref.10). The cross section of this reaction and the exact $E\Theta^2$ distribution of the π°'s are not known experimentally.

To study this background, we must discriminate between showers induced by π°'s (or γ's) and by electrons. This is possible by using the information of the shower scanner and of the forward detector :

- Fig.9 shows the number of photoelectrons measured by the shower scanner in the first half radiation length ($\sim$ 24cm) of the shower.We have assumed that the shower scanner consists of 4 rows of PM's each of them with 8 PM/meter and aligned along the corners of the tank. A cut keeping 50% of the electrons retains 10% of the γ rays.

- The 2 γ rays of a π° have a minimal angle of 270 mrad/ E(GeV). The photons are often separated in the forward detector leading to a ratio E_{peak}/E_T incompatible with the electron hypothesis (Fig.10). If one of the photons misses the forward detector and if the pair is not too asymmetric, the ratio E_{For}/E_T is different from the standard electron value. A cut retaining 90% of the electrons removes half of the π°'s.

When both shower scanner and forward detector informations are combined, taking into account their correlation, a cut keeping 45% of the electrons rejects 94% of the π^o's.

III-4 ν_e Interactions.

a) ν_e-Nucleon interactions

The neutral current ν_e interactions on nucleons and the ν_e charged current interactions in which the electron misses the forward detector are rejected with the same efficiency as neutral current ν_μ-N interactions. Since the ν_e flux is only 2% of the ν_μ flux this background is negligible.

Charged current events with an electron in the forward direction, including quasielastic events, are a more severe background. However, since the ν_e's have higher energies than ν_μ's in the wide band beam, a cut on the electron energy (E_e < 40 GeV) reduces this background by a factor 5.Moreover, the $E\,\theta^2$ distribution of the remaining ν_e-N events is flat in the angular acceptance of the forward detector. The expected signal to background ratio is $\simeq$ 16.

b) ν_e-e interactions

The ν_e-e $\rightarrow \nu_e$e cross section is $\sim$ 10 times higher than the ν_μe $\rightarrow \nu_\mu$e cross section. Since ν_e-e charged or neutral currents are indistinguishable from ν_μ-e events this contribution has to be statistically substracted. Knowing the ν_e flux with a precision of 10%, we are left with a possible contamination of the ν_μ-e signal of $\sim$ 2%. Selecting electrons outside the ν-e kinematical limit ($E\,\theta^2$ >2 MeV) provide an almost pure sample of ν_e-N interactions to monitor the ν_e flux.

III-5 Summary of backgrounds.

Table 1 shows the expected signal and backgrounds for a detector of 400 tons fiducial mass and 10^{18} protons on target in the neutrino case. The overall signal to background ratio is > 7 .

III-6 y dependence of the $\nu_\mu e$ signal.

For a fixed electron energy, the y distribution ($y=E_e/E_\nu$) depends on the coupling constants g_L and g_R and on the beam energy spectrum S(E) as:

$$dN/dE_e\, dy = \text{const} \times S(E_e/y) \times (1/y) \times [g_L^2 + g_R^2 (1-y)^2]$$

Since $y = 1-E_e\,\theta_e^2/2m_e$, the y distribution is equivalent to the $E_e\,\theta_e^2$ distribution. This distribution is shown in fig.11 for different values of the electron energy.

It is striking that for low energy electrons ($E_e < 10$ GeV) there is a dip at small values of $E\theta^2$. Thanks to our good angular resolution this dip is not washed out by the smearing (see Fig. 12). This behaviour can be very useful:

-To check the $E\theta^2$ dependence of the background making sure that it is really flat.

-To allow the detection of phenomena like γ's at $\theta=0°$ etc...

-To give an additional constrain on the determination of the coupling constants.

IV-THE EXPERIMENT.

IV-1 Experimental set-up.

The general design of the detector follows directly from the detection principles outlined in detail before. A tentative solution is sketched in fig.13 . Assuming a useful beam diameter of 4m, the transverse dimension of the water volume will have to be about 6 x 6m^2. The length of the detector should be $\sim$ 40m to obtain a fiducial mass of $\sim$ 400 tons. Veto counters in front of the detector will tag incoming muons. Final state muons will be identified and measured with a CDHS-type spectrometer.

To limit cost and size of the mirrors, the optical system for the angular measurement (windows, mirrors and focal plane detectors) will be subdivided in several identical modules, each of them viewing $\sim$ 8m length in the beam direction. There will be two detectors per module (one on top and one at the side) to measure the two orthogonal projections of the angle. The mirrors will extend over the full lateral width of the tank but will be only 3m high. The focal plane detectors ($\sim$ 150 phototubes each) will cover an area of 1.6 x 1.6 m^2.

For the total energy measurement, the fiducial volume will be surrounded by 2 phototubes (5" diameter) per m^2. The four corners of the tank will be equipped with shower scanners (cf.II-4).

The detailed design of the apparatus will depend on the outcome of engineering studies which are not yet completed. We are also investigating alternative design principles. For example, the delicate windows could be suppressed completely at the expense of doubling the horizontal width of the tank, imaging the horizontal angle measurement via a large plane mirror installed under 45° inside the water volume (Fig.14). The forward Cerenkov light is then viewed through the free water surface, which is inclined by 40 mrad with respect to the beam axis, by two detection systems mounted side by side on top of the tank.

To establish the validity of the proposed detection principles and to investigate the performances of all detector elements, we plan an extensive test with a small size prototype detector exposed to the X5 test beam during the period P5, 1983. The final design of the setup will have to await the result of this test which will be available by beginning of 1984.

A preliminary cost estimate is based on the design as shown in fig.13. Per 8m detector length (100 tons fiducial mass), we estimate :

- optical system :	120 KSF
- photomultiplier with electronics and mounting :	480 KSF
- water tank	30 KSF
TOTAL (8m length)	630 KSF

An overhead for floor space, infrastructure, on-line computer etc.... is not included in this estimate. Also, we envisage to borrow as much equipment as possible from completed experiments.

IV-2 Running time-Flux monitoring.

The questions of the flux monitoring and of the running time depend upon the method used to measure $\sin^2\theta_W$.

The first method is the measurement of the ratio R= $(\bar{\nu}_\mu e)/(\nu_\mu e)$ with 5% accuracy.This can be achieved with 1300 $\nu_\mu e$ and 1300 $\bar{\nu}_\mu e$ events corresponding to 4 10^{18} protons and 8 10^{18} protons on target, respectively. These numbers were obtained with a 7 GeV cut on the electron energy. This is a rather conservative cut and we hope the our forthcoming test will show that it is possible to decrease this cut below 5 GeV. The advantages of this method are clear : the systematics due to the cut on the electron energy and the detector efficiency cancel in the ratio $\nu/\bar{\nu}$. However, it is necessary to know the relative normalization of ν and $\bar{\nu}$ exposures. It can be obtained using the quasielastic ν_μ-N events. These events have a clear signature in our detector, but it remains to be proven that ν and $\bar{\nu}$ cross sections are equal of the level of a few percent.

A second possibility is to measure only the $\nu_\mu e$ cross section but with an accuracy of 2.5%. This requires a total of 8 10^{18} p.o.t. The absolute flux could be monitored (for ν energies above 10.8 GeV) by the inverse μ decay reaction $\nu_\mu e \to \mu \nu_e$ which has a cross section ~ 10 times larger than the $\nu_\mu e \to \nu_\mu e$ reaction. Also here the experimental signature is very clear : a narrow peak in the $E\theta^2$ distribution of the muons above the flat background of quasielastic events. This method requires however an extrapolation of the flux below 10.8 GeV and the precise knowledge of the absolute efficiency of the detector.

A third complementary method uses the capability of our detector to measure the $E\,\theta^2$ distribution for different electron energies. The energy distribution of the beam has to be known and can be measured with inverse muon decay and quasielastic interactions. The main difficulty with this last method is the accurate determination of the θ_e- error and consequently the y error. The validity of the method depends strongly on the achievable precision of the y measurement which will be investigated in the forthcoming test.

CONCLUSION.

In conlusion, we have presented a new detector design to measure $\nu_\mu e$ scattering with an angular accuracy of 5 mrad/$\sqrt{E}$, $\sim$ 6 times smaller than the kinematical limit.

The good resolution allows an analysis of the y distribution. The knowledge of this distribution permits a better determination of the poorly known backgrounds and gives an additional constraint on the measurement of $\sin\theta^2_w$.

Clearly, since such a type of detector is entirely new, many experimental points remain to be checked. We hope that the forthcoming test with a small size prototype will prove the feasability of the proposed detector.

Table 1

Event type	ν_μ NC	ν_μ CC	ν_e, $\bar{\nu}_e$ CC	$\nu_\mu e$
Rate for 10^{18} p.o.t. 400 T Fid. Vol.	10^6	$4\ 10^6$	$8.5\ 10^4$	560
E_{For}/E_T, E_{Peak}/E_{For} $7 < E_T < 40$	< 120	< 120	2500 500	530 350
$E\ \theta^2$ cut	< 12	< 12	20	320

REFERENCES

- 1 A. BLONDEL and F. JACQUET , Int. Rep. LPNHE (X 82-04) June 1983
A. BLONDEL et al. , SPS Workshop (Dec. 1982)

- 2 J.F. WHEATER and C.H. LLEWELYN SMITH , Nucl. Phys. B 208 (1982) 27

- 3 M. JONKER et al. (CHARM Collab) , Phys. Letters 117B (1982) 272

- 4 CHARM II Proposal , CERN SPSC (83-24) (April 1983)

- 5 P. FAYET , XVIIth Rencontre de Moriond ,1982 .Vol.1,483 (J.Tran Thanh Van Ed.)

- 6 L. BEHR et al. , Nucl. instr. methods 190 (1981), 5

- 7 J.W. CRONIN and M.L. SWARTZ , Fermilab Proposal 600 , Mai 1978

- 8 L. SULAK , Neutrino Conf. 81 (E. Fiorini Ed.)
R.M. BIONTA et al. , XVIIth Rencontre de Moriond, 1982, Vol.1,447 (J.Tran Thanh Van Ed.)

- 9 A. BLONDEL and F. JACQUET , Physics Letters 117B(1982) 115

- 10 D. REIN and L. SEHGAL , Nucl. Phys., to be published.

FIGURE CAPTIONS.

Fig.1 Forward detector principle

Fig.2 Projected angle of shower particles distribution for several electron energies.

Fig.3 Universal curve, $(1/E_e)\ dN/d\theta_z$, number of photoelectrons emitted by an electron shower as a function of the projected angle.

Fig.4 Distribution of the difference between the measured value (obtained as the maximum of each distribution) and the true value θ_z .

Fig.5 Angular resolution of the space angle as a function of the shower energy.

Fig.6 Sketch of the shower scanner.

Fig.7 Scatter plot of the ratios E_{For}/E_T versus E_{Peak}/E_{For} for e, π^+, π° shower.

Fig.8 Scatter plot of the ratios E_{For}/E_T versus E_{Peak}/E_{For} for e and neutral current shower.

Fig.9 Number of detected photoelectrons, from the first part of the showers for e and γ rays.

Fig.10a Typical π° signal

Fig.10b E_{Peak}/E_T distribution for e and π°

Fig.11 $E\theta^2$ distributions per bin of electron energy.

Fig.12 Same distribution as 11 but with the smearing due to an angular resolution of $5\text{mrad}/\sqrt{E}$

Fig.13 General layout of the detector.

Fig.14 Layout of a detector without window.

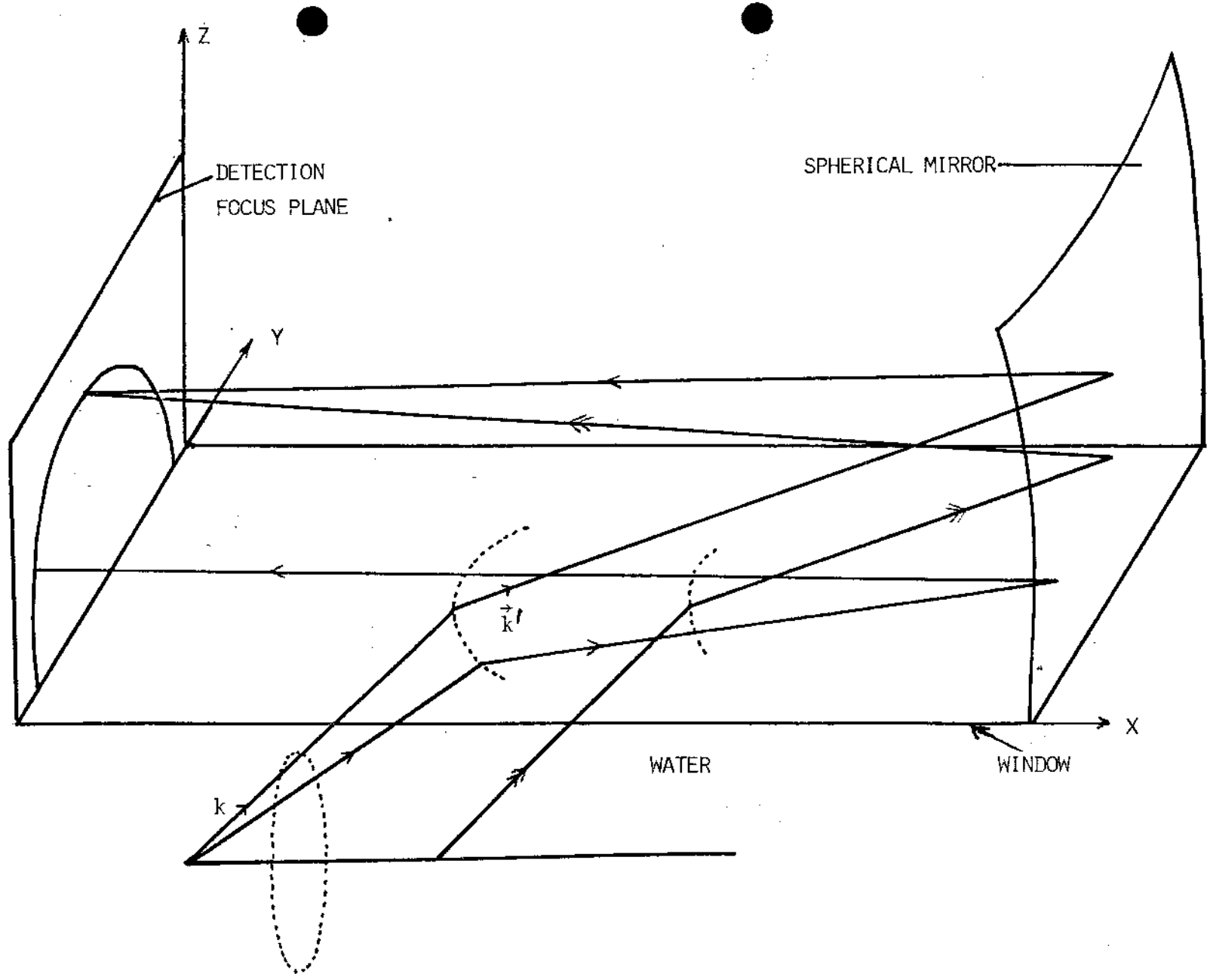

FIG 1 . FORWARD DETECTOR PRINCIPLE

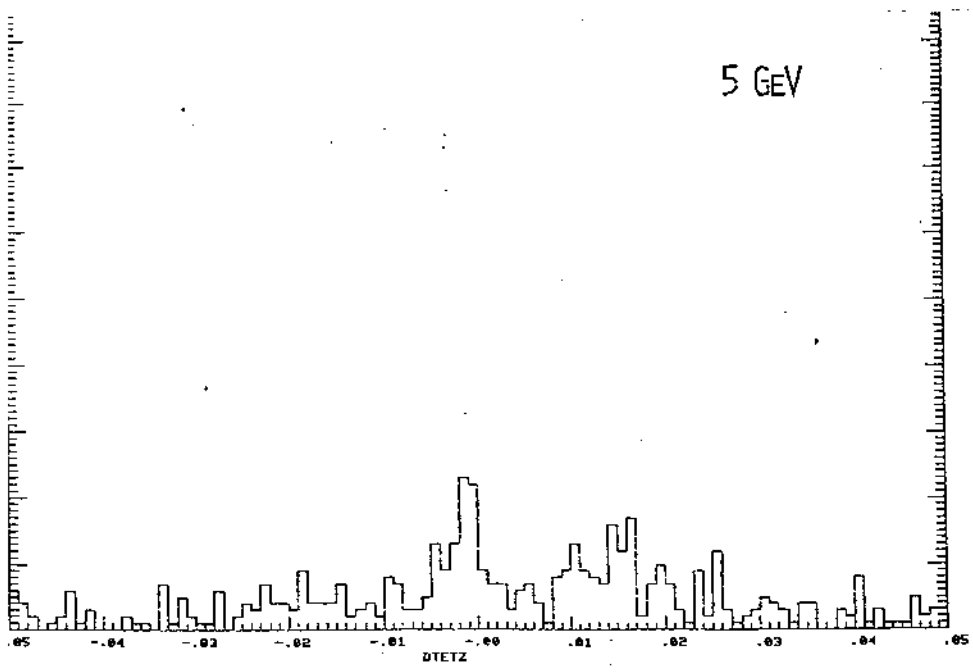

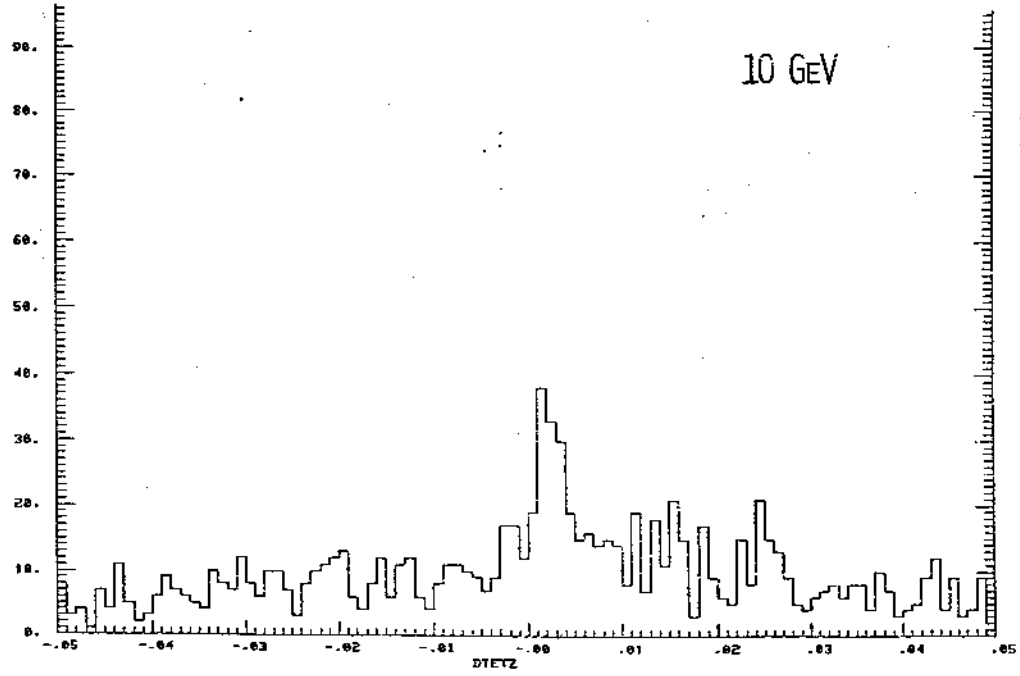

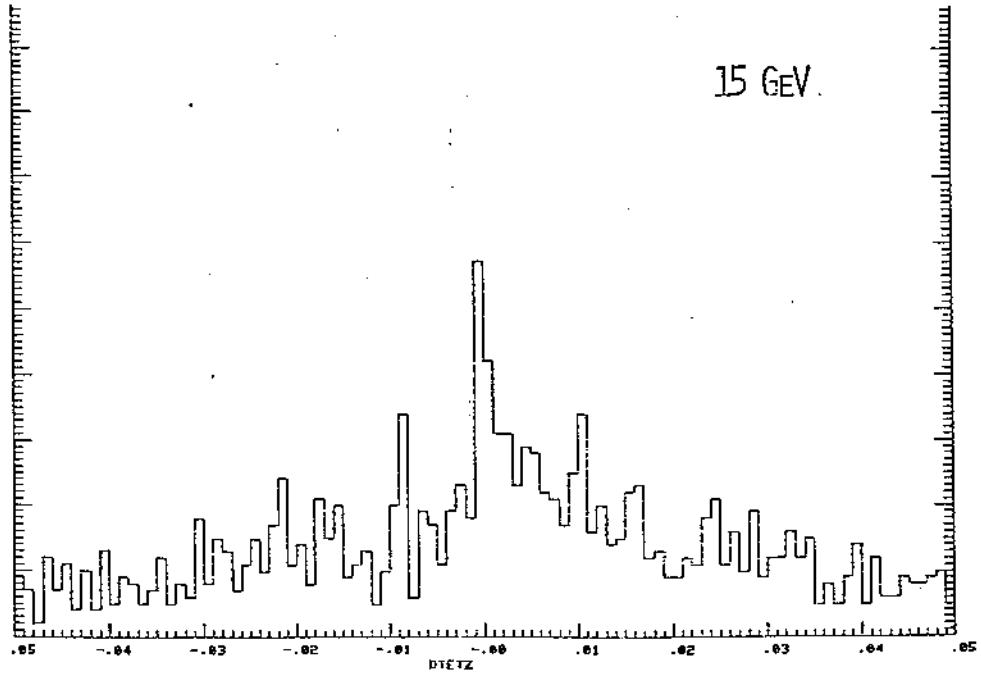

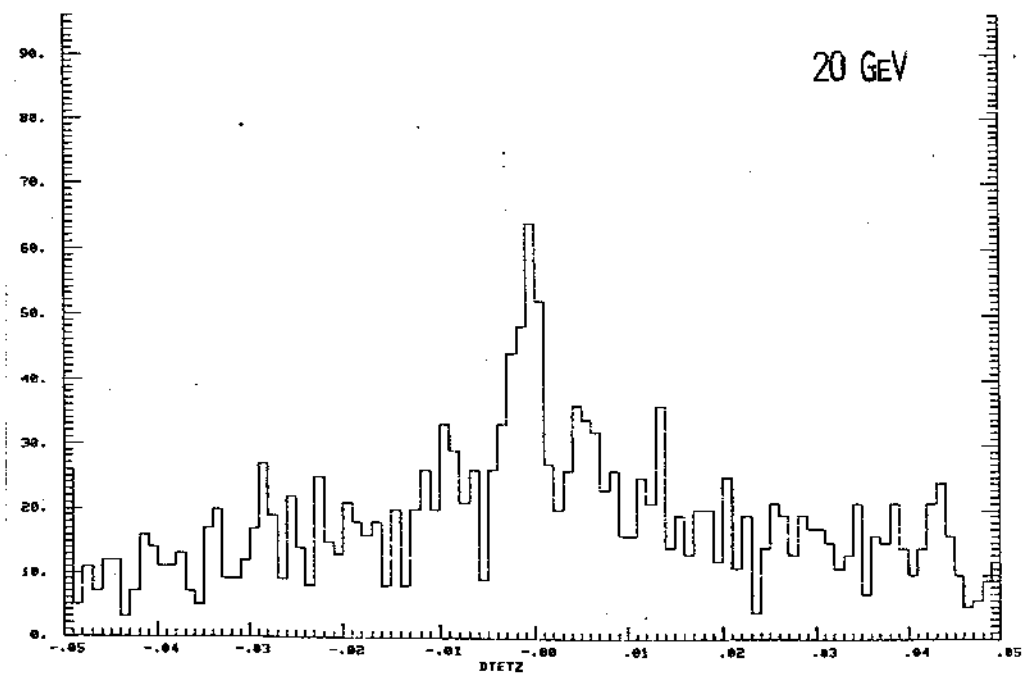

FIGURE 2

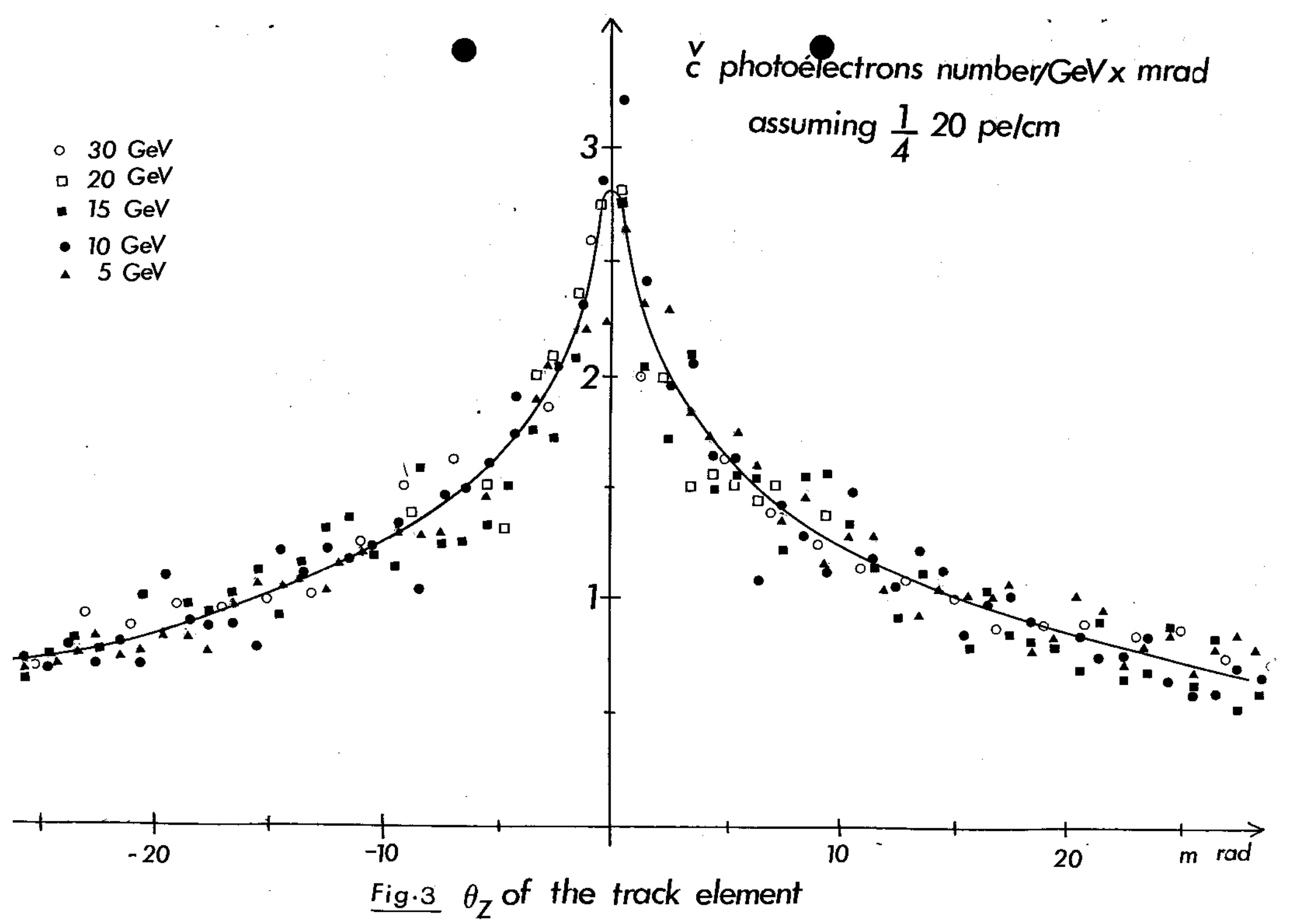

Fig·3 θ_Z of the track element

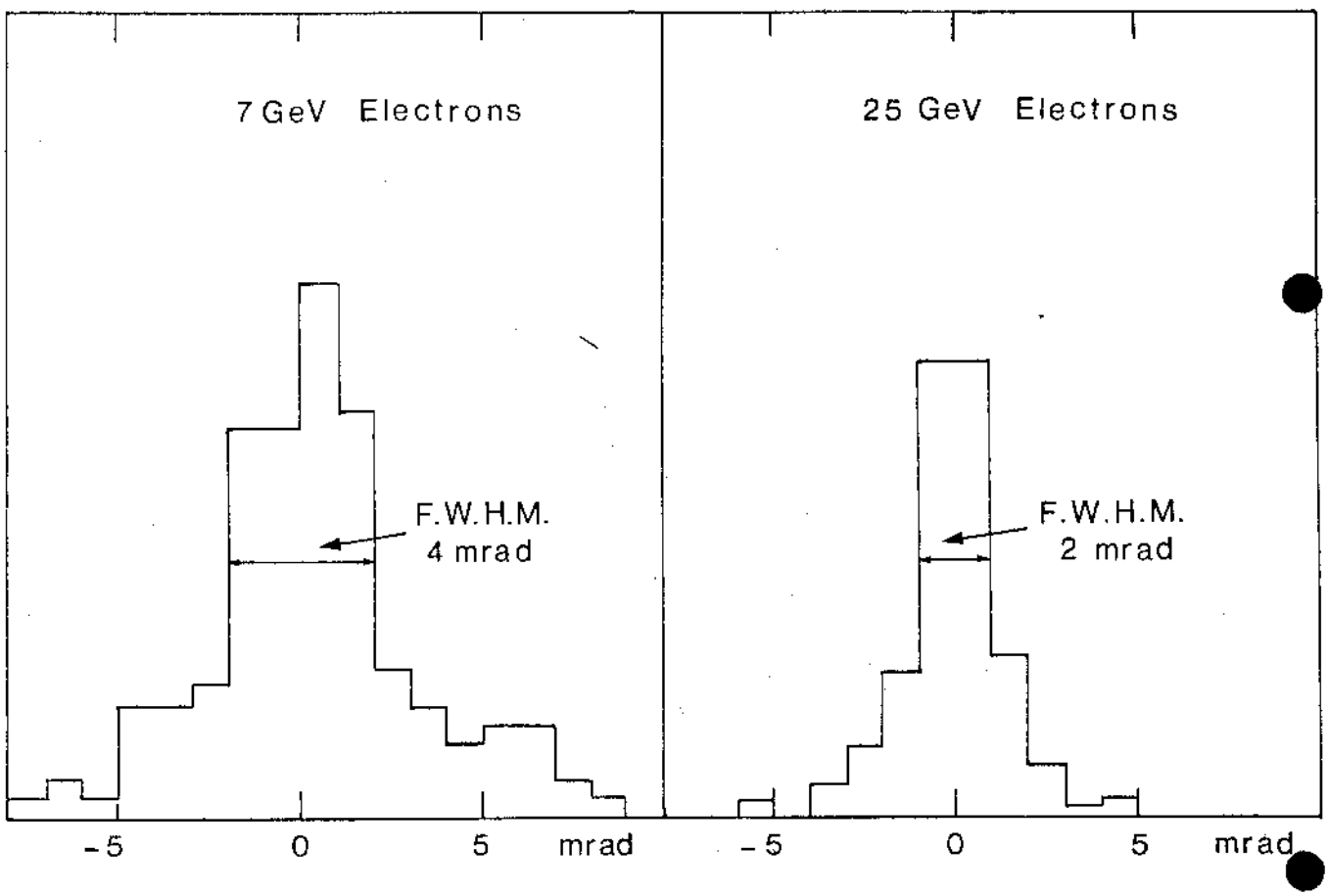

$$\theta_z^{meas} - \theta_z^{true}$$

Fig.4

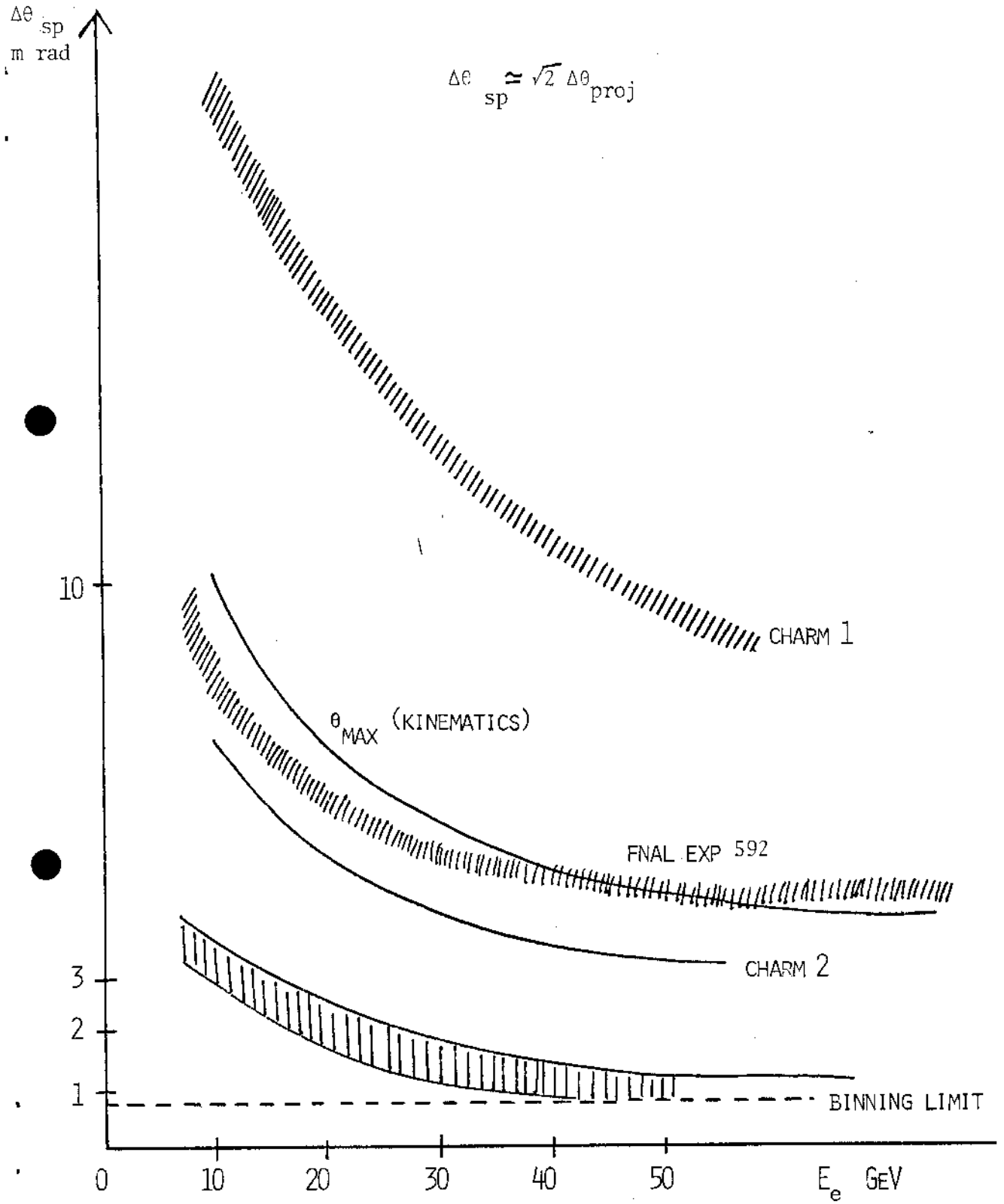

FIG. 5 - ANGULAR RESOLUTION

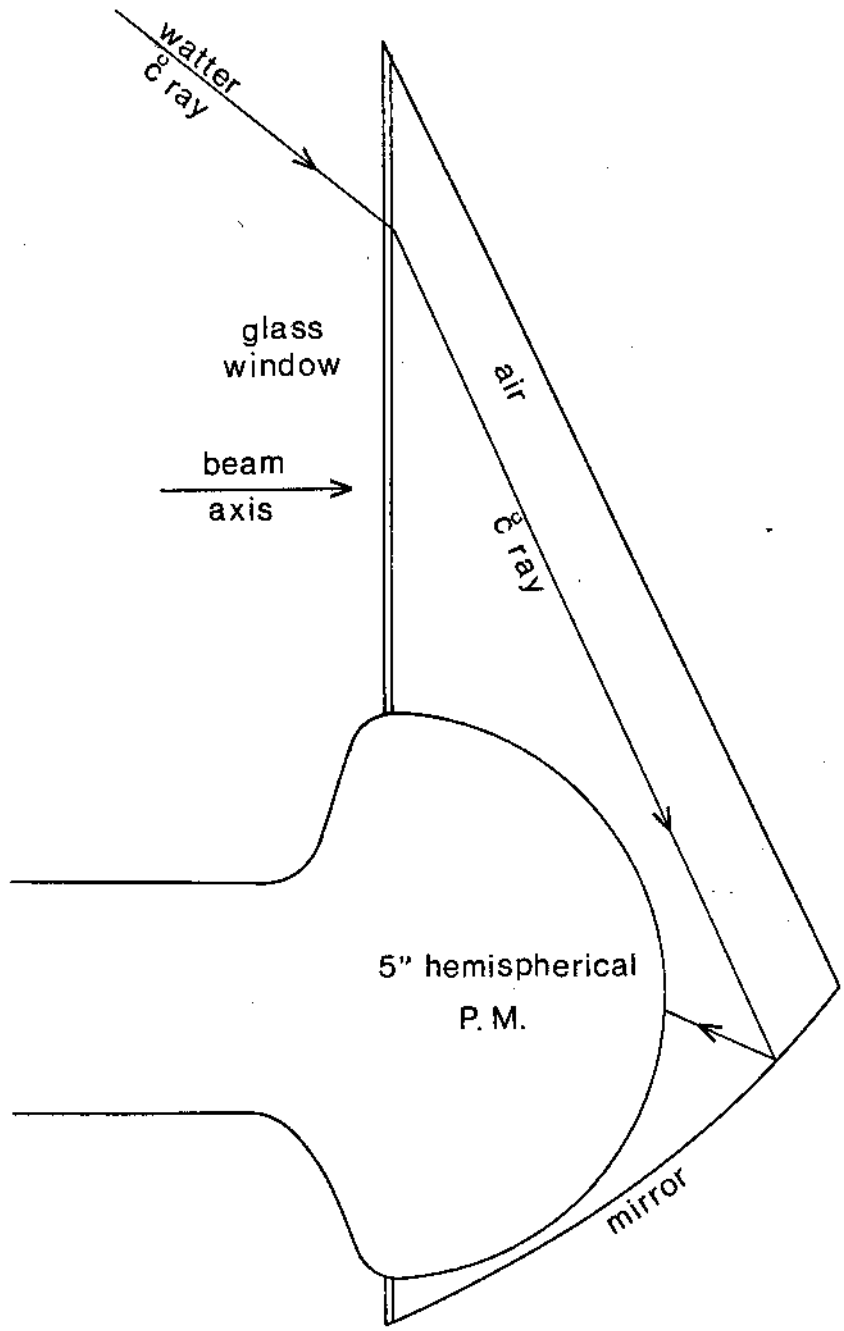
watter
c ray
glass
window
beam
axis
air
c ray
5" hemispherical
P. M.
mirror

Fig.6

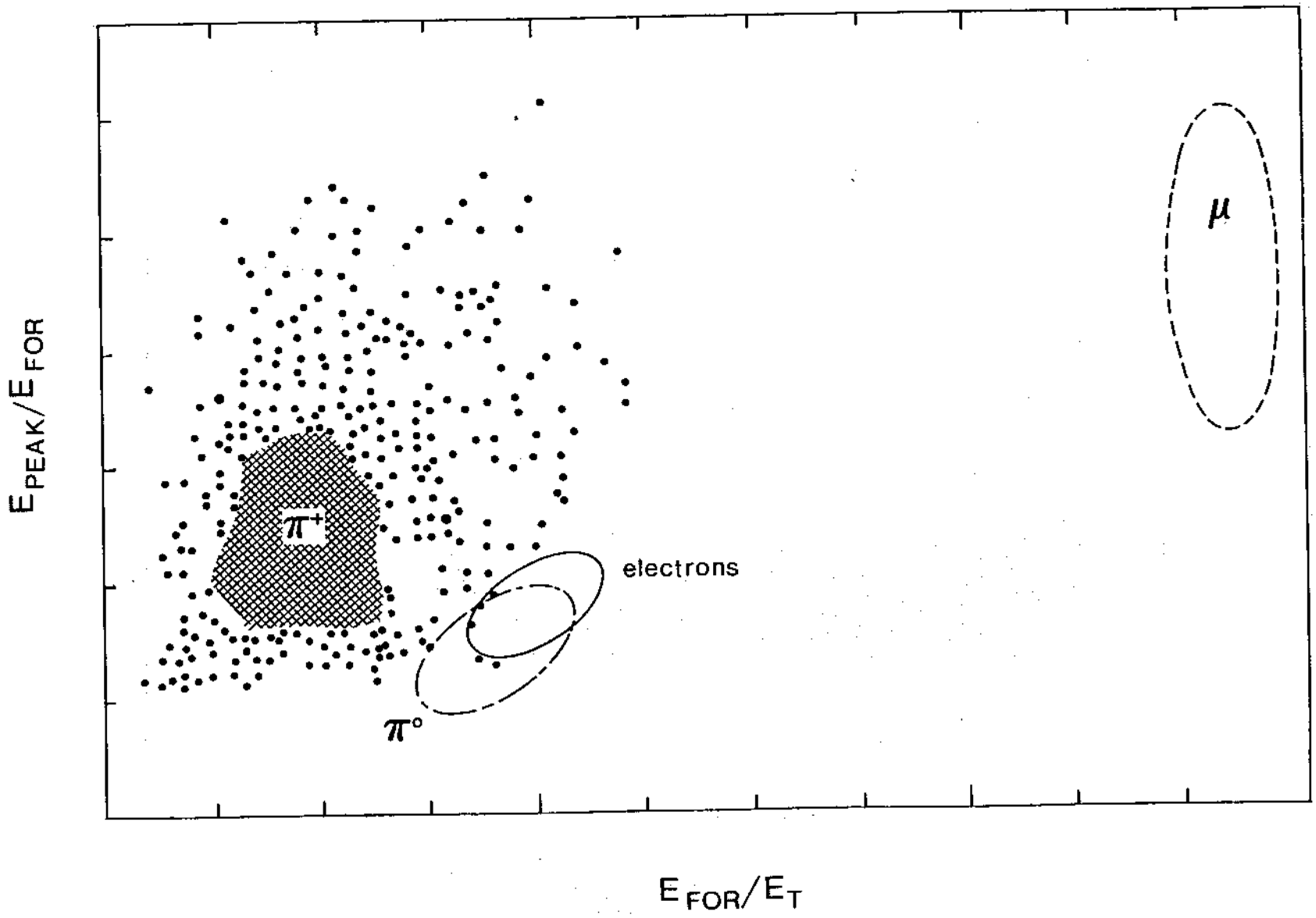

Fig. 7

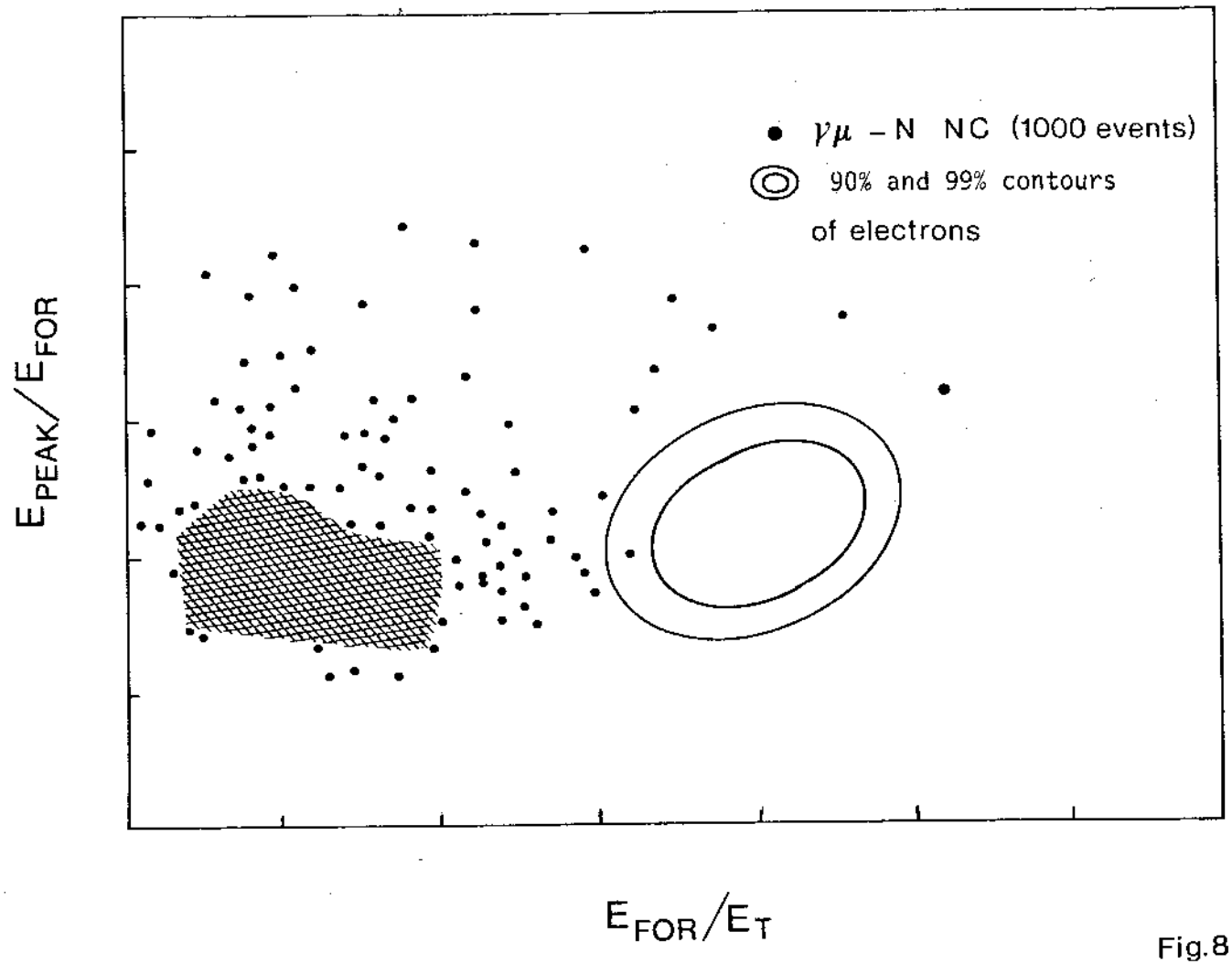
$\nu\mu$ – N NC (1000 events)
90% and 99% contours
of electrons
E_{PEAK}/E_{FOR}
E_{FOR}/E_T

Fig.8

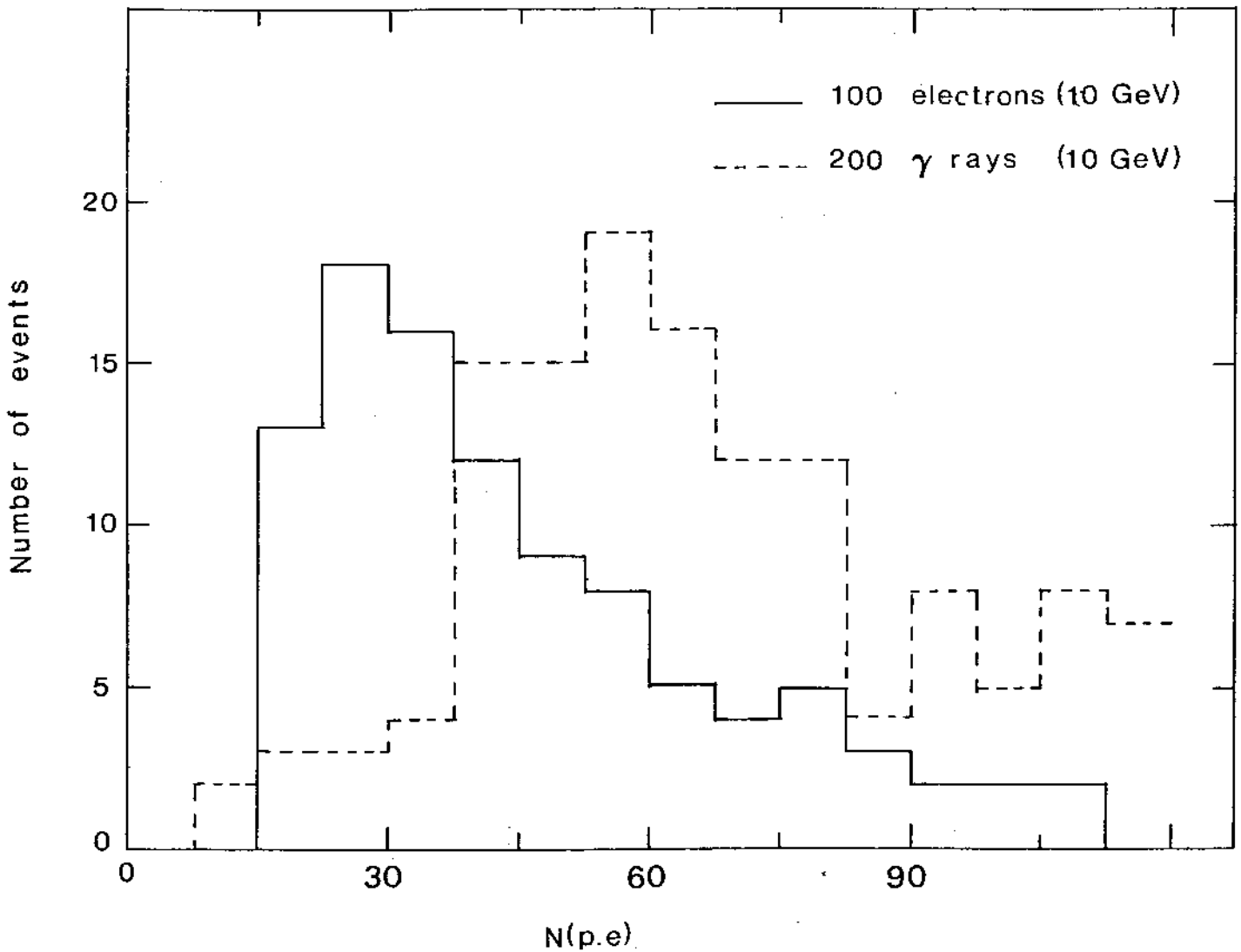
100 electrons (10 GeV)
200 γ rays (10 GeV)
Number of events
0
5
10
15
20
0
30
60
90
N(p.e)

Fig. 9

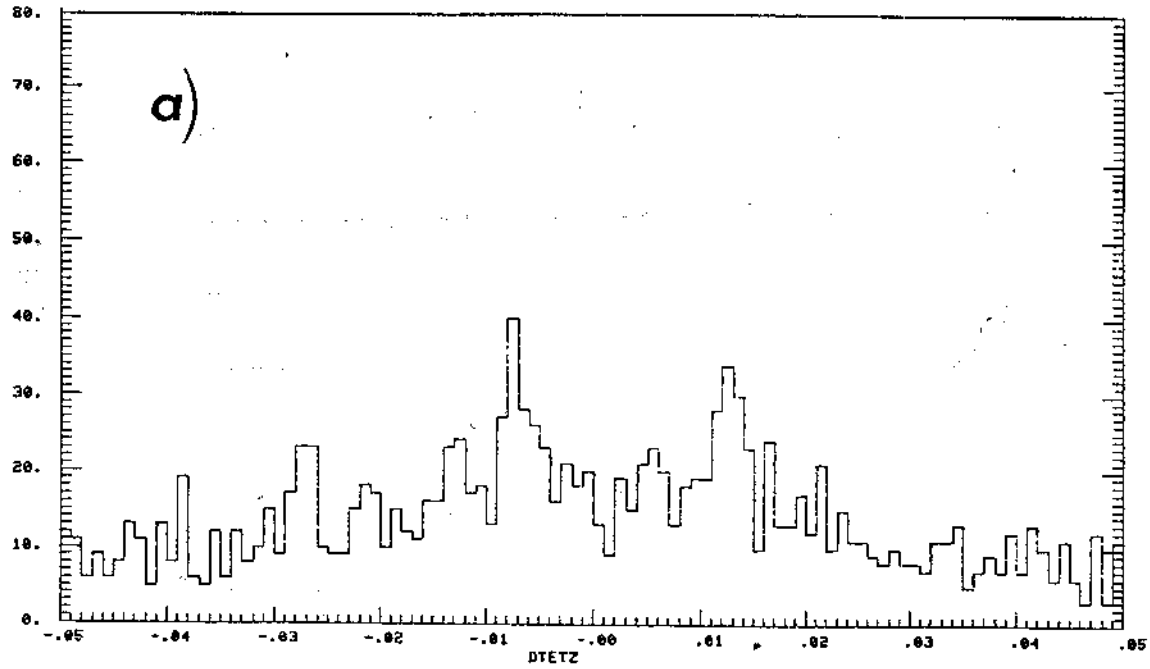
a)
80.
70.
60.
50.
40.
30.
20.
10.
0.
-.05
-.04
-.03
-.02
-.01
-.00
.01
.02
.03
.04
.05
DTETZ

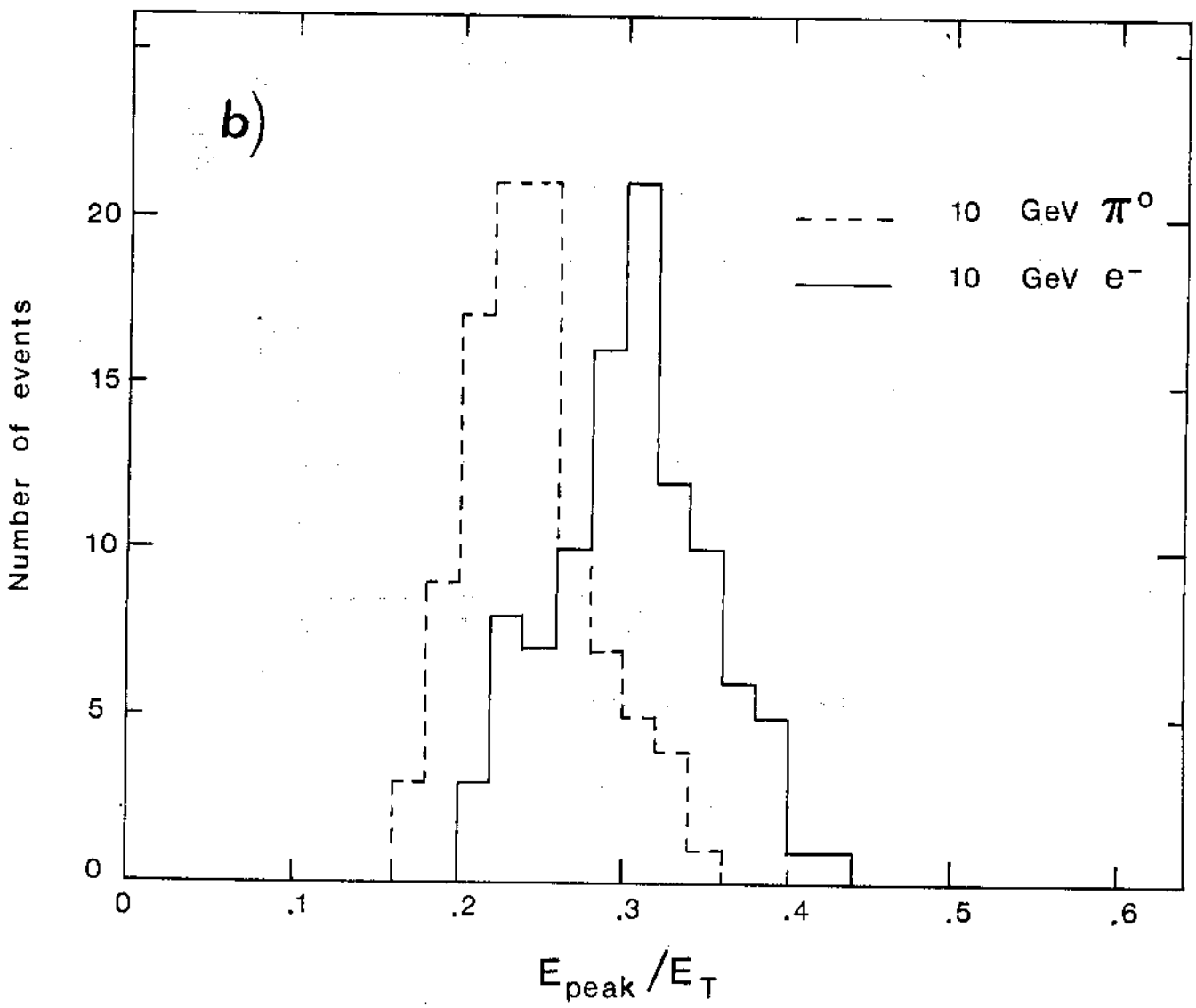
b)
10 GeV π°
10 GeV e⁻
Number of events
20
15
10
5
0
0
.1
.2
.3
.4
.5
.6
E peak /E T

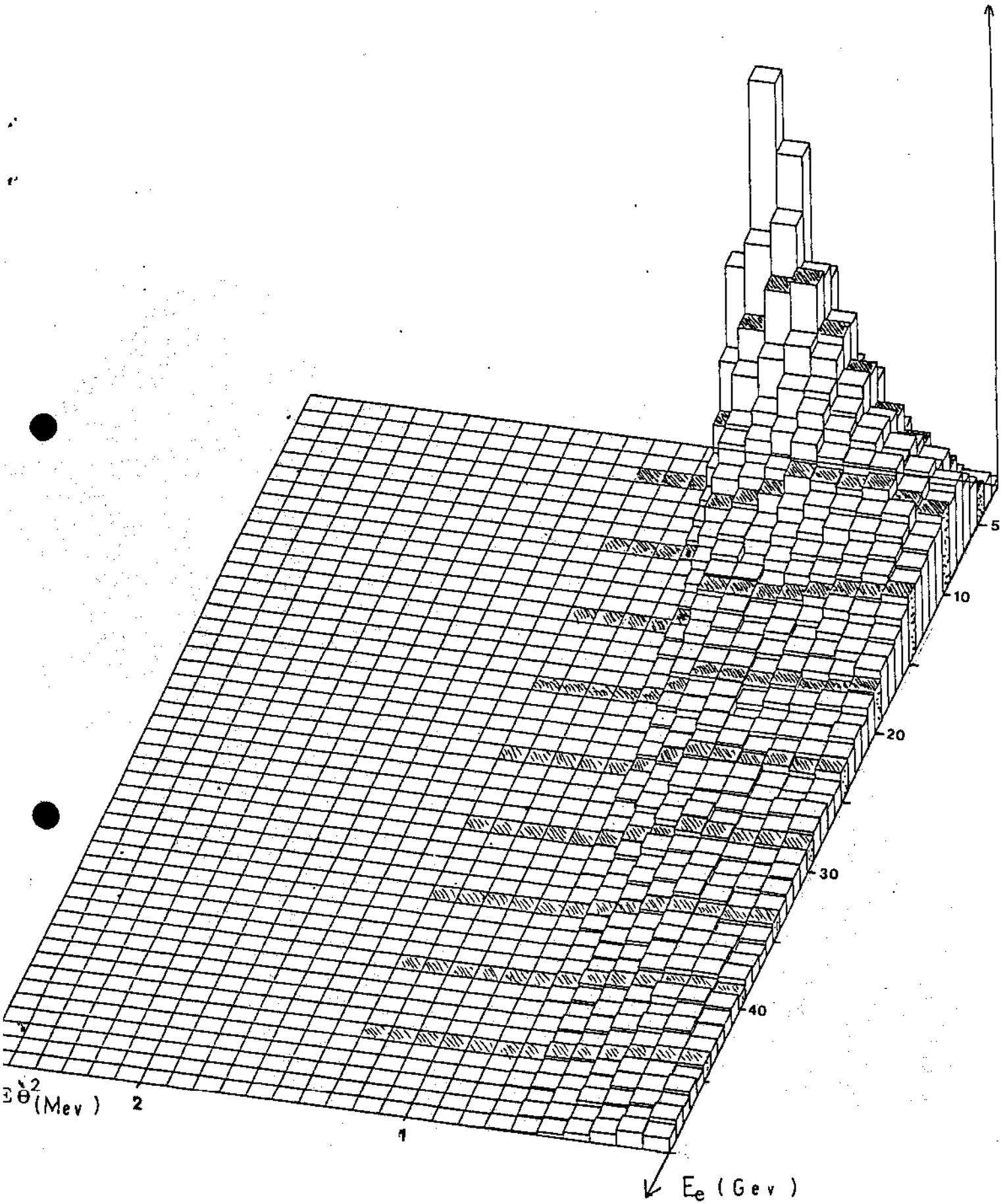

fig. 11

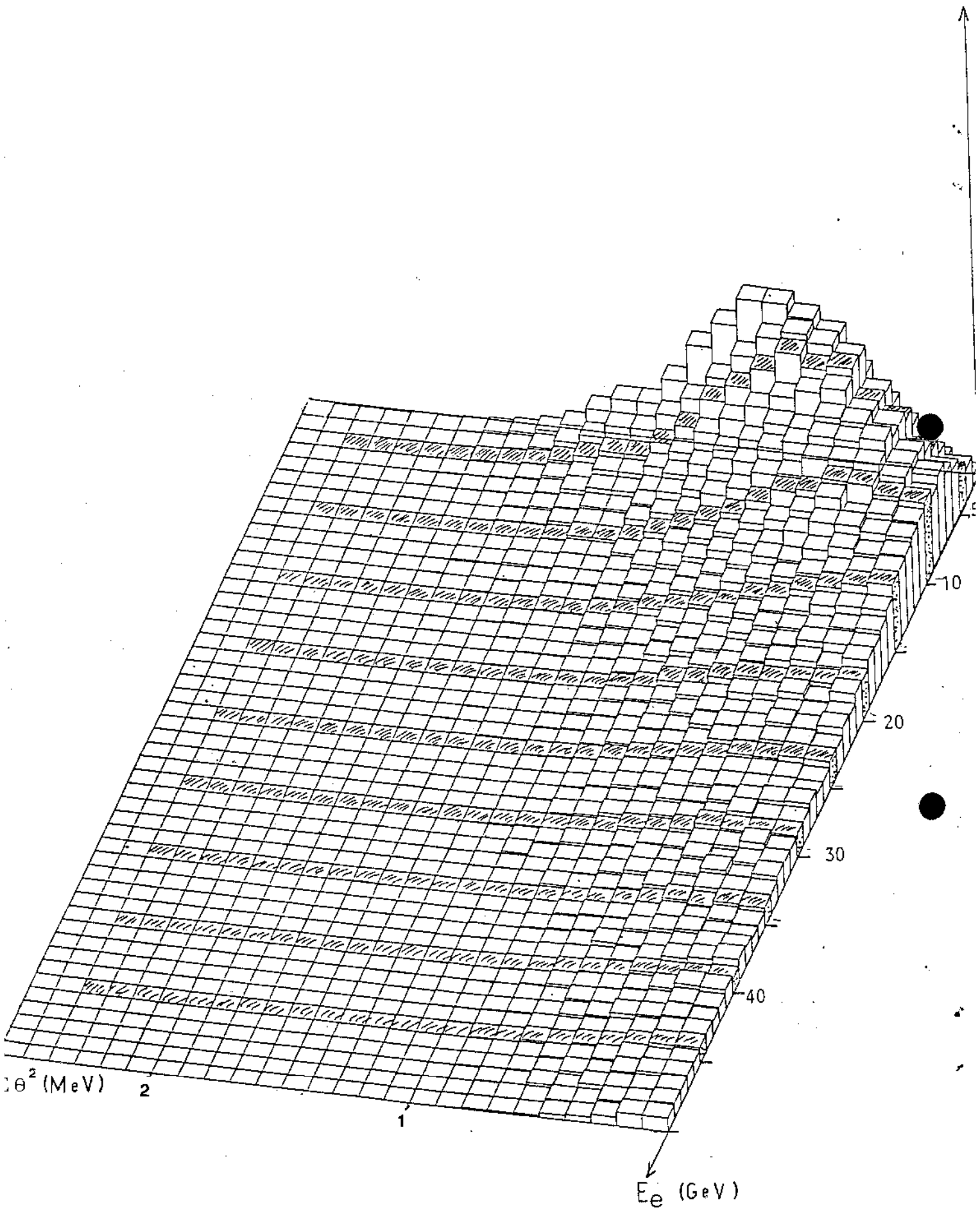

fig. 12

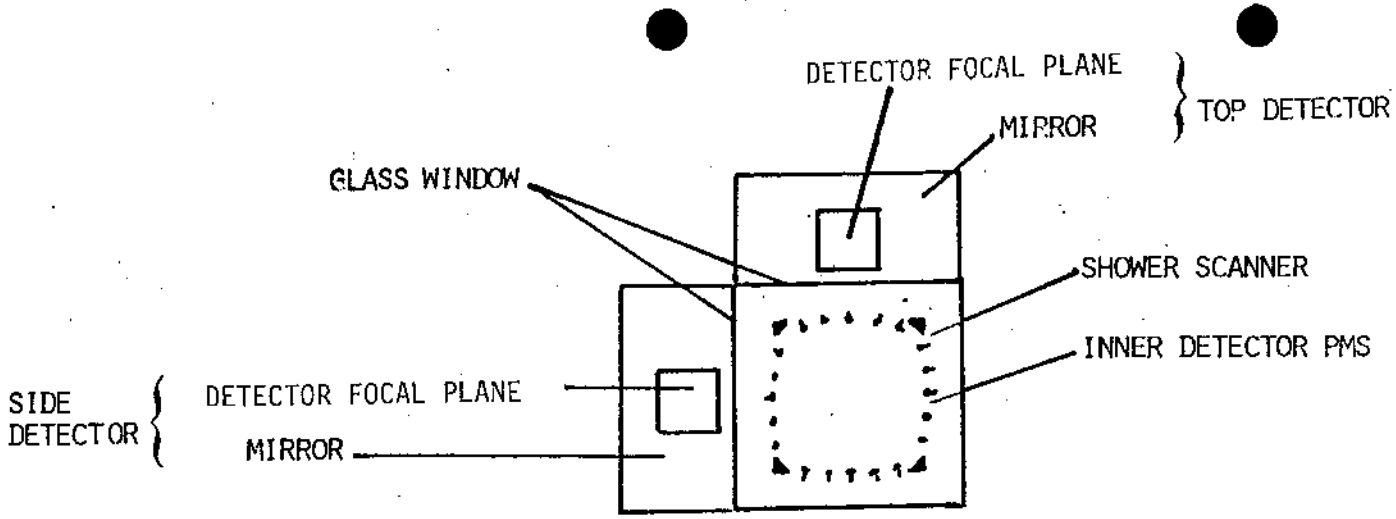

FIG 13A TRANSVERSE CUT

FIG 13B LONGITUDINAL CUT

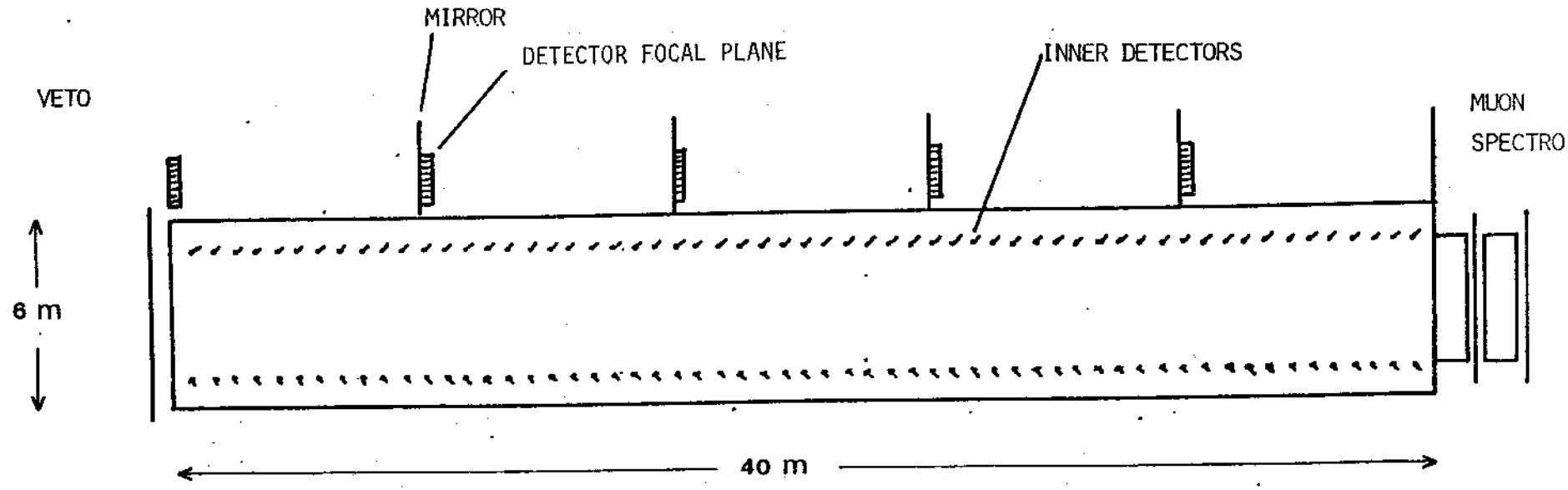

FIG 13 . GENERAL LAYOUT OF THE DETECTOR

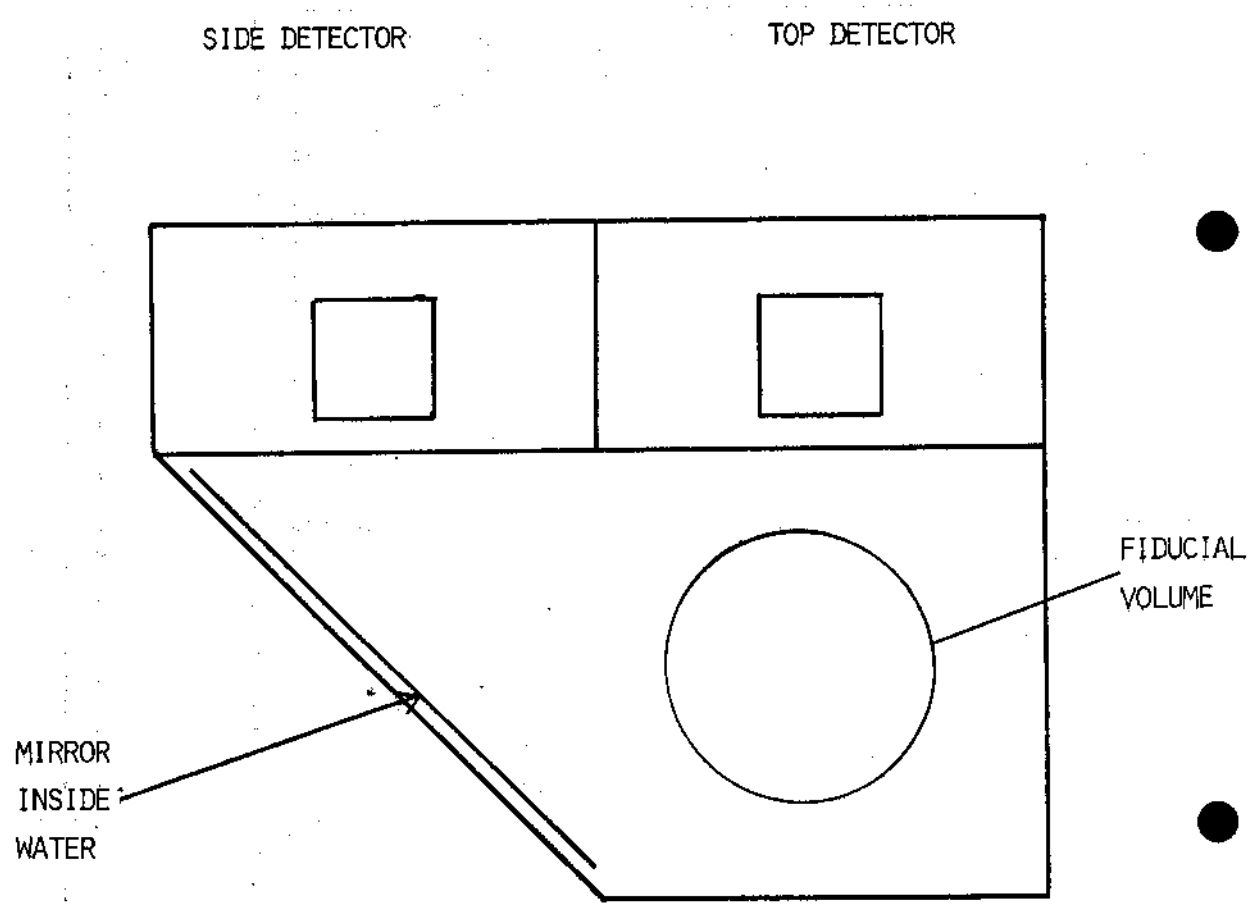

FIG 14. LAYOUT OF A DETECTOR WITHOUT WINDOW